Crowded Cu(I) Complexes Involving Benzo[*h*]quinoline: π-Stacking Effects and Long-Lived Excited States

Elvira C. Riesgo, Yi-Zhen Hu, Frédéric Bouvier, and Randolph P. Thummel*

Department of Chemistry, University of Houston, Houston, Texas 77204-5641

Donald V. Scaltrito and Gerald J. Meyer

Department of Chemistry, Johns Hopkins University, Baltimore, Maryland 21218

Received March 19, 2001

The Friedländer condensation was employed to synthesize two series of 3,3′-polymethylene bridged ligands, L, based on 2-(2′-pyridyl)-benzo[*h*]quinoline and 2,2′-bibenzo[*h*]quinoline (BHQ) along with the fully aromatic naphtho[1,2-*b*]-1,10-phenanthroline. Complexes $[Cu(L)_2]^+$ were prepared as their perchlorate or hexafluorophosphate salts. The solution state structures were analyzed by NMR and shielding effects reflected significant interligand π-stacking interaction in the complexes. Solid-state structures of the complexes where L = 3,3′-tetramethylene-2,2′-bibenzo[*h*]quinoline or naphtho[1,2-*b*]-1,10-phenanthroline were determined by X-ray analysis. The tetramethylene bridged complex showed a highly distorted coordination geometry with the BHQ rings of opposing ligands π-stacked at a interplanar distance of about 3.37 Å. Complexes of the BHQ series showed a pronounced MLCT absorption maximum which shifted bathochromically from 496 to 610 nm as the 3,3′-bridge decreased from 4 to 2 carbons. The BHQ complexes luminesced strongly in CH_2Cl_2 solution and the tetramethylene-bridged system showed the longest yet recorded excited-state lifetime for a copper MLCT excited state, $\tau = 5.3$ μs and $\Phi = 0.10$.

Introduction

The manner in which a ligand controls the properties of its metal complexes depends on a combination of steric, electronic, and conformational effects. A thorough understanding of these effects will assist in the rational design of complexes with specific and predictable properties.[1] Complexes of Cu(I) are well suited to this type of study since their redox, electron transfer, and optical behavior is highly dependent upon the nature of the ligands.[2]

Investigations with 1,10-phenanthroline (**1a**, phen) and, to a lesser extent, 2,2′-bipyridine (bpy) have demonstrated that substituents in the *ortho*-positions have a stabilizing effect on the Cu(I) state where the ligands lie in approximately orthogonal planes. Upon oxidation to Cu(II), the complex tends toward square planar geometry which would force both ligands into the same plane, a process which is severely impeded by *ortho*-substituents. Recent studies by McMillin and co-workers[3] and also Karpishin and co-workers[4] have methodically investigated this effect for a variety of different size substituents.

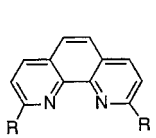

1 a R = H
b R = CH_3

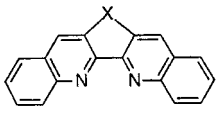

2 a X = H, H
b X = $(CH_2)_2$
c X = $(CH_2)_3$
d X = $(CH_2)_4$

Electronic effects can also play an important role such that more electronically delocalizing or electronegative ligands can provide a lower energy π^* state and thus decrease the energy of the metal-to-ligand charge transfer (MLCT) transition, allowing the chromophore to harvest visible light. This delocalizing effect has been demonstrated by comparing complexes such as $[Cu(\mathbf{1b})_2]^+$ and $[Cu(\mathbf{2})_2]^+$ where the more electronegative 2,2′-biquinoline (**2**) accounts for an approximately 100 nm bathochromic shift in the MLCT band.[5] For a series of 3,3′-bridged derivatives of 2,2′-biquinoline (**2a**−**d**), we have recently shown that the conformation of the ligand, controlled by twisting about the 2,2′-bond, can also have a profound effect on the properties of the complex.[5] The following study will reemphasize the importance of such conformational effects for a series of highly congested benzo[*h*]quinoline (BHQ) ligands.

(1) (a) Kalyanasundaram, K. *Photochemistry of Polypyridine and Porphyrin Complexes*; Academic Press: San Diego, CA, 1992. (b) Juris, A.; Balzani, V.; Barigelletti, F.; Campagna, S.; Belser, P.; Von Zelewsky, A. *Coord. Chem. Rev.* **1988**, *84*, 85. (c) Meyer, T. J. *Acc. Chem. Res.* **1989**, *22*, 163. (d) Crosby, G. A. *J. Chem. Educ.* **1983**, *60*, 791.

(2) (a) Miller, M. T.; Karpishin, T. B. *Inorg. Chem.* **1999**, *38*, 5246. (b) Cunningham, C. T.; Moore, J. J.; Cunningham, K. L. H.; Fanwick, P. E.; McMillin, D. R. *Inorg. Chem.* **2000**, *39*, 3638. (c) Miller, M. T.; Gantzel, P. K.; Karpishin, T. B. *Inorg. Chem.* **1998**, *37*, 2285. (d) Meyer, M.; Albrecht-Gary, A.; Dietrich-Buchecker, C. O.; Sauvage, J. *Inorg. Chem.* **1999**, *38*, 2279. (e) Eggleston, M. K.; Fanwick, P. E.; Pallenberg, A. J.; McMillin, D. R. *Inorg. Chem.* **1997**, *36*, 4007. (f) Pallenberg, A. J.; Koenig, K. S.; Barnhart, D. M. *Inorg. Chem.* **1995**, *34*, 2833. (g) Navon, N.; Golub, G.; Cohen, H.; Paoletti, P.; Valtancoli, B.; Bencini, A.; Meyerstein, D. *Inorg. Chem.* **1999**, *38*, 3484. (h) Kutal, C. *Coord. Chem. Rev.* **1990**, *99*, 213. (i) Horvath, O. *Coord. Chem. Rev.* **1994**, *135*, 303−324. (j) Scaltrito, D. V.; Thompson, D. W.; O'Callahan, J. A.; Meyer, G. J. *Coord. Chem. Rev.* **2000**, *208*, 243.

(3) Eggleston, M. K.; McMillin, D. R.; Koenig, K. S.; Pallenburg, A. J. *Inorg. Chem.* **1997**, *36*, 172.

(4) Miller, M. T.; Gantzel, P. K.; Karpishin, T. B. *Inorg. Chem.* **1999**, *38*, 3414.

(5) Jahng, Y.; Hazelrigg, J.; Kimball, D.; Riesgo, E.; Wu, F.; Thummel, R. P. *Inorg. Chem.* **1997**, *36*, 5390.

10.1021/ic010297h CCC: $20.00
Published on Web 05/30/2001

An important consequence of sterically encumbering a Cu(I) diimine complex has been the realization of longer excited-state lifetimes. For example, Karpishin et al. have reported a 730 ns excited-state lifetime for the heteroleptic compound $[Cu(dtbp)(dmp)]^+$ (dtbp = 2,9-di-*tert*-butyl-phen, dmp = 2,9-dimethyl-phen).[6] Using a similar approach, McMillin et al. have recently reported that $[Cu(dbtmp)_2]^+$ (dbtmp = 2,9-di-*n*-butyl-3,4,7,8-tetramethyl-phen) had a lifetime of 920 ns in CH_2Cl_2.[7] In the excited state, the metal is formally a d9 Cu(II) center that is subject to a Jahn−Teller distortion. This leads to a tetragonally distorted geometry in the emissive state, with the two phen ligands being nearly coplanar. Substituents in the 2,9-positions inhibit this structural change and force the excited state into a more tetrahedral environment.[3,4] This destabilization of the excited state increases the energy gap between the Cu *d*-orbitals and the π^* orbitals of the ligands, thereby slowing nonradiative decay. Coordination compounds exhibiting such long-lived photoluminescent excited states at ambient temperature are finding applications as chemical sensors[8] and biological probes.[9]

In this study, two closely related series of ligands have been prepared, 2-(2′-pyridyl)-benzo[*h*]quinolines **3a**−**d** and 2,2′-bibenzo[*h*]quinolines **5a**−**c**, and the optical and redox properties of Cu(I) complexes derived from them have been characterized. The ligands may be considered as naphtho[1,2-*b*]-fused derivatives of bpy where the two azaaryl halves of the molecule are bridged at the 3,3′-positions by polymethylene units which control the dihedral angle between the two halves. Along with **4**, the aromatized analogue of **3b**, these ligands combine steric, electronic, and conformational effects, all of which will influence a coordinated metal. In a steric sense, the coordinating bpy-like pocket of ligands **3a**−**d** is congested by the fused naphtho-ring whose H10 points almost directly toward the metal binding site. For ligands **5a**−**c**, this effect is doubled by the presence of two such rings. Initially, we suspected that this latter series of ligands would not allow access to a metal. In an electronic sense, the naphtho-rings dramatically enhance the ability of the ligand to delocalize charge and thus contribute to increased electronegativity. Finally, the length of the polymethylene bridge influences the conformation of the molecule and consequently the geometry around a bound metal in both the ground and excited states. Electronic communication through the 2,2′-bond will likewise be affected.

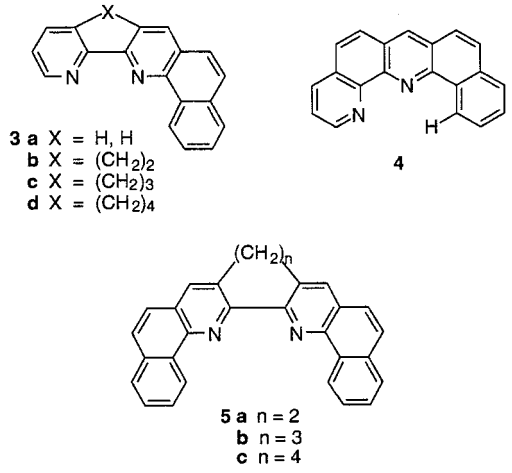

Experimental Section

Melting points were obtained on a Hoover capillary melting point apparatus and are uncorrected. Cyclic voltammograms were recorded using a BAS CV-27 Voltammograph and a Houston Instruments Model 100 X-Y recorder according to a procedure which has been previously described.[10] Elemental analyses were performed by National Chemical Consulting, P.O. Box 99, Tenafly, NJ 07670. CH_3CN was refluxed over CaH_2 and then distilled under Ar. The 1,2-cycloheptanedione,[11] 1,2-cyclooctanedione,[12] 8-oxo-5,6,7,8-tetrahydroquinoline,[13] cyclohepta-[*b*]-pyridin-9-one,[13] cycloocta[*b*]pyridin-10-one,[13] naphtho[1,2-*b*]-1,10-phenanthroline,[14] 1-amino-2-naphthaldehyde,[15] and $[Cu(CH_3CN)_4]$-ClO_4[16] were prepared according to reported procedures.

2-(2′-Pyridyl)-benzo[*h*]quinoline (3a). To a solution of 2-acetylpyridine (69 mg, 0.6 mmol) and 8-amino-7-quinolinecarbaldehyde (**7**, 100 mg, 0.58 mmol) in absolute EtOH (10 mL) was added saturated ethanolic KOH (0.5 mL). The solution was refluxed under Ar for 17 h. After evaporation of the solvent, the residue was purified by chromatography on alumina (20 g), eluting with CH_2Cl_2/hexanes (1:3), to provide **3a** (110 mg, 75%) as yellow crystals, mp 104−105 °C: ^{1}H NMR (CD_3CN) δ 9.42 (d, 1H, J = 9.0 Hz, H_{10}), 8.86 (d, 1H, J = 9.0 Hz, $H_{3'}$), 8.72 (d, 1H, J = 3.0 Hz, $H_{6'}$), 8.68 (d, 1H, J = 9.0 Hz, H_3), 8.38 (d, 1H, J = 9.0 Hz, H_4), 7.98 (dd, 1H, J = 6.0 Hz, H_7), 7.96 (dd, 1H, $H_{4'}$), 7.88 (AB quartet, 1H, J = 9.0, 15.0 Hz, H_5 or H_6), 7.80 (AB quartet, 1H, J = 9.0, 15.0 Hz, H_5 or H_6), 7.77 (m, 2H, H_8/H_9), 7.43 (dd, 1H, J = 6.0 Hz, $H_{5'}$); ^{13}C NMR ($CDCl_3$) δ 156.7, 154.4, 149.0, 146.0, 137.1, 136.8, 134.0, 131.9, 128.3, 128.1, 128.0, 127.1, 126.6, 125.4, 124.7, 124.0, 122.0, 119.4.

3,2′-Dimethylene-2-(2′-pyridyl)-benzo[*h*]quinoline (3b). Following the procedure described for **3a**, 8-oxo-5,6,7,8-tetrahydroquinoline (**6b**, 84 mg, 0.6 mmol) was condensed with **7** (100 mg, 0.58 mmol) in absolute EtOH. The crude product was chromatographed on alumina (20 g), eluting with CH_2Cl_2/hexanes (4:1), to give **3b** (120 mg, 75%) as a beige solid, mp 173−174 °C: ^{1}H NMR (CD_3CN) δ 9.35 (d, 1H, J = 9.0 Hz, H_{10}), 8.72 (d, 1H, J = 6.0 Hz, $H_{6'}$), 8.12 (s, 1H, H_4), 7.98 (dd, 1H, J = 9.0 Hz, H_7), 7.87 (AB quartet, 1H, J = 6.0 Hz, H_5 or H_6), 7.81−7.69 (m, 4H), 7.35 (dd, 1H, J = 6.0 Hz, $H_{5'}$), 3.17 (m, 2H, H_α), 3.06 (m, 2H, $H_{\alpha'}$); ^{13}C NMR (CD_3CN) δ 152.4, 151.0, 149.5, 146.2, 136.3, 135.2, 134.5, 133.6, 132.5, 132.0, 128.5, 128.3, 127.8, 127.1, 126.6, 125.7, 124.8, 123.8, 28.1, 28.0. Anal. Calcd for $C_{20}H_{14}N_2 \cdot 0.25H_2O$: C, 83.77; H, 5.06; N, 9.77. Found: C, 83.67; H, 4.69; N, 9.73.

3,2′-Trimethylene-2-(2′-pyridyl)-benzo[*h*]quinoline (3c). Following the procedure described for **3a**, cyclohepta-[*b*]-pyridin-9-one (**6c**, 200 mg, 1.24 mmol) was condensed with **7** (216 mg, 1.28 mmol) in absolute EtOH. An oily solid was isolated which when triturated with Et_2O (10 mL) gave **3c** (263 mg, 71%) as yellow crystals, mp 160−162 °C: ^{1}H NMR (CD_3CN) δ 9.24 (dd, 1H, J = 9.0 Hz, H_{10}), 8.74 (dd, 1H, J = 3.0 Hz, $H_{6'}$), 8.19 (s, 1H, H_4), 8.00 (d, 1H, J = 9.0 Hz, H_7), 7.92 (AB quartet, 1H, J = 6.0 Hz, H_5 or H_6), 7.82 (AB quartet, 1H, J = 6.0, 15.0 Hz, H_5 or H_6), 7.77−7.72 (m, 3H), 7.41 (dd, 1H, J = 4.5 Hz, $H_{5'}$), 2.72 (t, 2H, J = 6.9 Hz, H_α), 2.56 (t, 2H, J = 6.9 Hz, $H_{\alpha'}$), 2.27 (m, 2H, H_β); ^{13}C NMR (CD_3CN) δ 157.5, 156.6, 148.8, 148.8, 145.9, 136.7, 135.6, 133.6, 131.9, 128.4, 128.1, 127.8, 127.1, 126.3, 125.6, 124.9, 124.9, 123.6, 32.1, 30.1, 30.0. Anal. Calc for $C_{21}H_{16}N_2$: C, 85.14; H, 5.40; N, 9.46. Found: C, 85.26; H, 5.55; N, 9.30.

3,2′-Tetramethylene-2-(2′-pyridyl)-benzo[*h*]quinoline (3d). Following the procedure described for **3a**, cycloocta[*b*]pyridin-10-one (**6d**, 154 mg, 0.88 mmol) was condensed with **7** (150 mg, 0.88 mmol) in

(6) Miller, M. T.; Gantzel, P. K.; Karpishin, T. B. *J. Am. Chem. Soc.* **1999**, *121*, 4292.
(7) Cunningham, C. T.; Cunningham, K. L. H.; Michalec, J. F.; McMillin, D. R. *Inorg. Chem.* **1999**, *38*, 4388.
(8) Xu, W.; McDonough, R. C.; Langsdorf, B.; Demas, J. N.; DeGraff, B. A. *Anal. Chem.* **1994**, *66*, 4133.
(9) Lakowicz, J. R.; Malak, H.; Grycynski, I.; Castellano, F. N.; Meyer, G. J. *Biospectroscopy* **1995**, *1*, 163.
(10) Goulle, V.; Thummel, R. P. *Inorg. Chem.* **1990**, *29*, 1767.
(11) Vanderhear, R. W.; Voter, R. C.; Banks, C. V. *J. Org. Chem.* **1949**, *14*, 836.
(12) Wittig, G.; Krebs, A. *Chem. Ber.* **1961**, *44*, 3760.
(13) Thummel, R. P.; Lefoulon, F.; Cantu, D.; Mahadevan, R. *J. Org. Chem.* **1984**, *49*, 2208.
(14) Wu, F.; Riesgo, E. C.; Pavalova, A.; Kipp, R. A.; Schmehl, R.; Thummel, R. P. *Inorg. Chem.* **1999**, *38*, 5620.
(15) Riesgo, E. C.; Jin, X.; Thummel, R. P. *J. Org. Chem.* **1996**, *61*, 3017.
(16) Hemmerich, P.; Sigwart, C. *Experentia* **1963**, 488.

absolute EtOH. After concentration of the solution, the residual brown oil was diluted with CH_2Cl_2, washed with water, and dried over $MgSO_4$. After evaporation of the solvent, the residue was chromatographed on silica gel, eluting first with CH_2Cl_2 to remove unreacted starting materials, then with EtOH/CH_2Cl_2 (1:1) to afford **3d** (210 mg, 77%): ^{1}H NMR ($CDCl_3$) δ 9.36 (d, 1H, J = 5.4 Hz, H_{10}), 8.72 (d, 1H, J = 3.9 Hz, $H_{6'}$), 8.05 (s, 1H, H_4), 7.87 (d, 1H, J = 5.7 Hz, H_7), 7.80 (d, 1H, J = 8.7 Hz, H_5), 7.66 (m, 3H, $H_{4'}$, H_8 and H_9), 7.60 (d, 1H, J = 8.7 Hz, H_6), 7.37 (dd, 1H, $H_{5'}$), 2.97 (q, 1H, J = 5.7 Hz, H_α), 2.76 (q, 1H, J = 5.7 Hz, $H_{\alpha'}$), 2.40 (t, 2H, J = 11.7 Hz, H_β), 2.25 (q, 1H, J = 11.7 Hz, H_α), 2.15 (t, 2H, J = 11.7 Hz, $H_{\beta'}$), 1.65 (q, 1H, J = 11.7 Hz, $H_{\alpha'}$); ^{13}C NMR ($CDCl_3$) δ 156.8, 156.1, 147.6, 145.1, 138.1, 137.6, 136.6, 136.4, 133.5, 131.7, 128.1, 128.0, 127.7, 126.9, 126.6, 125.4, 124.8, 123.9, 31.7, 30.4, 29.4.

Naphtho[1,2-*b*]-1,10-phenanthroline (4). To a solution of 3,2′-dimethylene-2-phenyl-1,10-phenanthroline (**3b**, 220 mg, 0.78 mmol) in nitrobenzene (5 g), Pd/C (100 mg, 10%) was added. The suspension was refluxed under Ar for 24 h, at which time a second portion of Pd/C (25 mg, 10%) and nitrobenzene (1 g) were added. Reflux was continued for another 24 h. The hot solution was filtered through Celite and the Celite was rinsed with CH_2Cl_2 (3 × 10 mL). Concentration of the filtrate gave a thick liquid which was chromatographed on alumina (20 g) eluting first with CH_2Cl_2/hexanes (1:1) to provide unreacted **3b** and then with $CHCl_3$ to obtain an oily solid. This solid was washed with Et_2O/hexanes (1:1) to give **4** (100 mg, 46%) as a beige solid, mp 198−200 °C: ^{1}H NMR (CD_3CN) δ 9.63 (d, 1H, J = 9.0 Hz, $H_{9'}$), 9.20 (dd, 1H, J = 3.0 Hz, H_9), 8.90 (s, 1H, H_4), 8.40 (dd, 1H, J = 9.0 Hz, H_7), 8.07−7.82 (m, 7H), 7.76 (m, 1H, H_8); ^{13}C NMR ($CDCl_3$) δ 149.9, 149.8, 147.4, 146.2, 137.0, 135.4, 135.3, 134.0, 129.3, 129.1, 127.9, 127.7, 127.5, 127.4, 126.8, 126.7, 126.4, 126.0, 125.3, 123.4. Anal. Calcd for $C_{20}H_{12}N_2$: C, 85.71; H, 4.28; N, 10.00. Found: C, 85.65; H, 4.11; N, 9.87.

3,3′-Dimethylene-2,2′-bibenzo[*h*]quinoline (5a). To a solution of 1,2-cyclohexanedione (98 mg, 0.9 mmol) and 1-amino-2-naphthaldehyde (**7**, 300 mg, 1.75 mmol) in absolute EtOH (12 mL), 1 pellet of KOH was added. The solution was reluxed under Ar for 16 h. The light yellow precipitate was filtered and rinsed with cold EtOH (1 mL) to give **5a** (260 mg, 74%) as light yellow crystals, mp >280 °C: ^{1}H NMR ($CDCl_3$) δ 9.77 (d, 2H, J = 6.0 Hz, H_{10}), 8.02 (s, 2H, H_4), 7.94−7.86 (m, 4H), 7.77−7.71 (m, 2H), 7.84 (AB quartet, 2H, J = 9.0 Hz, H_5 or H_6), 7.67 (AB quartet, 2H, J = 9.0 Hz, H_5 or H_6), 3.30 (s, 4H, $-CH_2-$); ^{13}C NMR ($CDCl_3$) δ 151.2. 146.2, 134.7, 133.7, 133.4, 132.4, 128.6, 128.3, 127.9, 127.4, 126.7, 125.4, 125.0, 28.5. Anal. Calcd for $C_{28}H_{18}N_2$: C, 87.96; H, 4.71; N, 7.33. Found: C, 87.62; H, 5.05; N, 7.13.

3,3′-Trimethylene-2,2′-bibenzo[*h*]quinoline (5b). A solution of 1,2-cycloheptanedione (73 mg, 0.6 mmol), 1 mL saturated ethanolic KOH and **7** (200 mg, 1.17 mmol) in toluene (25 mL) was refluxed under Ar for 24 h using a Dean Stark water separator. The solution was then concentrated under vacuum, and the resulting solid was redissolved in CH_2Cl_2 (10 mL) and washed with H_2O (10 mL). The organic layer was dried ($MgSO_4$) and concentrated under reduced pressure to give an oily residue, which was washed with Et_2O (5 mL) to provide **5b** (90 mg, 38%) as a beige powder, mp > 280 °C: ^{1}H NMR ($CDCl_3$) δ 9.58 (d, 2H, J = 9.0 Hz, H_{10}), 8.09 (s, 2H, H_4), 7.94 (d, 2H, J = 9.0 Hz), 7.88 (AB quartet, 2H, J = 9.0 Hz, H_5 or H_6), 7.79−7.69 (m, 6H), 2.84 (t, 4H, J = 7.5 Hz, $-CH_2-$), 2.37 (quintet, 2H, J = 9.0 Hz, $-CH_2-$); ^{13}C NMR ($CDCl_3$) δ 157.0, 135.5, 134.0, 133.7, 132.2, 128.4, 128.1, 127.9, 127.2, 126.6, 125.3, 125.2, 125.0, 31.8, 30.3. Anal. Calcd for $C_{29}H_{20}N_2$·0.25H_2O: C, 86.89; H, 5.12; N, 6.99. Found: C, 87.09; H, 5.32; N, 6.79.

3,3′-Tetramethylene-2,2′-bibenzo[*h*]quinoline (5c). Following the procedure for **5b**, 1,2-cyclooctanedione (84 mg, 0.6 mmol) was condensed with **7** (200 mg, 1.16 mmol) in toluene (25 mL) to give **5c** (90 mg, 37%) as a beige powder, mp > 280 °C: ^{1}H NMR ($CDCl_3$) δ 9.42 (dd, 2H, J = 3.0 Hz, H_{10}), 8.11 (s, 2H, H_4), 7.92 (m, 2H), 7.84 (AB quartet, 2H, J = 9.0 Hz, H_5 or H_6), 7.74 (AB quartet, 2H, J = 9.0 Hz, H_5 or H_6), 7.68 (m, 4H), 3.00 (dd, 2H, J = 9.0 Hz, $-CH_2-$), 2.46 (t, 2H, J = 16.5 Hz, $-CH_2-$), 2.26 (t, 2H, J = 9.0 Hz, $-CH_2-$), 1.77 (t, 2H, J = 9.0 Hz, $-CH_2-$); ^{13}C NMR ($CDCl_3$) δ 157.0, 135.5, 134.0, 133.7, 132.2, 128.4, 128.1, 127.9, 127.2, 126.6, 125.3, 125.2, 125.0, 31.8, 30.8. Anal. Calcd for $C_{30}H_{22}N_2$·0.25H_2O: C, 86.85; H, 5.43; N, 6.75. Found: C, 87.01; H, 5.49; N, 6.67.

8,9,10,11-Tetrahydrobenzo-[*c*]-acridine (9). Following the procedure described for for **5a**, cyclohexanone (104 mg, 1.16 mmol) was condensed with **7** (200 mg, 1.16 mmol) in absolute EtOH (12 mL) to give **9** (117 mg, 43%) as a beige powder, mp 170 °C (dec): ^{1}H NMR ($CDCl_3$) δ 9.28 (d, 1H, J = 8.1 Hz, H_{10}), 7.86 (d, 1H, J = 8.1 Hz), 7.80 (s, 1H, H_4), 7.72−7.57 (m, 4H), 3.23 (t, 2H, J = 4.2 Hz, $-CH_2-$), 3.00 (t, 2H, J = 4.4 Hz, $-CH_2-$), 2.00 (m, 4H, $-CH_2-$); ^{13}C NMR ($CDCl_3$) δ 159.0, 150.0, 145.9, 144.2, 135.9, 135.3, 131.3, 128.2, 127.2, 126.2, 125.3, 122.4, 47.6, 35.4, 30.3, 28.2, 25.9. MS *m*/*e* 233.

[Cu(3a)$_2$]ClO$_4$. To a solution of 2-(2′-pyridyl)-benzo[*h*]quinoline (**3a**, 40 mg, 0.2 mmol) in CH_3CN (7 mL) was added solid [Cu(CH_3CN)$_4$]-ClO_4 (24 mg, 0.08 mmol). The purple solution was stirred under Ar for 2 h. Concentration of the solution gave [Cu(**3a**)$_2$]ClO_4 (54 mg, 100%) as purple crystals: ^{1}H NMR (CD_3CN) δ 8.72 (d, 2H, J = 6.0 Hz, H_{10}), 8.62 (d, 2H, J = 3.0 Hz, $H_{6'}$), 8.31 (d, 2H, J = 6.0 Hz, $H_{3'}$), 8.07 (t, 2H, J = 7.5 Hz, $H_{4'}$), 7.90 (broad s, 4H, H_3/H_4), 7.64 (d, 2H, J = 6.0 Hz, H_7), 7.59 (m, 2H, $H_{5'}$), 7.53 (AB quartet, 2H, J = 9.0 Hz, H_5 or H_6), 7.36 (m, 2H, H_8), 7.34 (AB quartet, 2H, J = 9.0 Hz, H_5 or H_6), 6.85 (t, 2H, J = 6.0 Hz, H_9). MS *m*/*e* 574 (M − ClO_4)$^+$.

[Cu(3b)$_2$]ClO$_4$. Following the procedure described for [Cu(**3a**)$_2$]-ClO_4, 3,2′-dimethylene-2-(2′-pyridyl)-benzo[*h*]quinoline (**3b**, 40 mg, 0.1 mmol) was treated with [Cu(CH_3CN)$_4$]ClO_4 (23 mg, 0.07 mmol) to give [Cu(**3b**)$_2$]ClO_4 (40 mg, 78%) as a purple powder: ^{1}H NMR (CD_3CN) δ 8.83 (broad s, 4H, $H_{6'}$/H_{10}), 8.01 (d, 2H, J = 6.0 Hz, $H_{4'}$), 7.79 (s, 2H, H_4), 7.64 (m, 6H), 7.47 (m, 2H, H_5 or H_6/H_8), 6.81 (broad s, 2H, H_9), 3.07 (broad s, 4H, $-CH_2-$), 2.95 (broad s, 4H, $-CH_2-$); MS *m*/*e* 625 (M − ClO_4)$^+$. Anal. Calcd for $C_{40}H_{28}N_4CuClO_4$: C, 66.02; H, 3.85; N, 7.70. Found: C, 66.22; H, 4.30; N, 7.60.

[Cu(3c)$_2$]ClO$_4$. Following the procedure described for [Cu(**3a**)$_2$]ClO_4, 3,2′-trimethylene-2-(2′-pyridyl)-benzo[*h*]quinoline (**3c**, 40 mg, 0.1 mmol) was treated with [Cu(CH_3CN)$_4$]ClO_4 (22 mg, 0.07 mmol) to give [Cu(**3c**)$_2$]ClO_4 (35 mg, 66%) as an orange powder: ^{1}H NMR (CD_3CN) δ 8.96 (d, 2H, J = 3.0 Hz, $H_{6'}$), 8.82 (d, 2H, J = 9.0 Hz, H_{10}), 7.93 (d, 2H, J = 9.0 Hz, $H_{4'}$), 7.81 (d, 2H, J = 9.0 Hz, H_7), 7.70 (m, 2H, $H_{5'}$), 7.72 (AB quartet, 2H, J = 9.0 Hz, H_5 or H_6), 7.42 (m, 4H, H_4/H_8), 7.40 (AB quartet, 2H, J = 9.0 Hz, H_5 or H_6), 7.02 (t, 2H, J = 7.5 Hz, H_9), 2.46 (t, 4H, J = 6.0 Hz, $-CH_2-$), 2.16 (s, H_2O), 2.06 (m, 4H, $-CH_2-$), 1.66 (broad s, 4H, $-CH_2-$); MS *m*/*e* 653 (M − ClO_4)$^+$. Anal. Calcd for $C_{42}H_{32}N_4CuClO_4$: C, 66.75; H, 4.23; N, 7.72. Found: C, 66.75; H, 4.04; N, 7.39.

[Cu(3d)$_2$]ClO$_4$. To a solution of 3,2′-tetramethylene-2-(2′-pyridyl)-benzo[*h*]quinoline (**3d**, 70 mg, 0.23 mmol) in CH_3CN (10 mL) and CH_2Cl_2 (5 mL) was added solid [Cu(CH_3CN)]ClO_4 (35.5 mg, 0.115 mmol). The mixture was stirred at 25 °C for 60 min and the solution was concentrated to afford [Cu(**3d**)$_2$]ClO_4 (61 mg, 68%) as a red crystalline powder: ^{1}H NMR (CD_3CN) δ 8.83 (d, 1H, J = 8.1 Hz, H_{10}), 8.68 (d, 1H, J = 4.5 Hz, $H_{6'}$), 7.85 (d, 1H, J = 7.8 Hz, H_5), 7.79 (d, 1H, J = 7.8 Hz, H_6), 7.71 (d, 1H, J = 8.7 Hz, H_7), 7.57 (dd, 1H, $H_{5'}$), 7.45 (t, 1H, J = 7.5 Hz, H_9), 7.40 (s, 1H, H_4), 7.38 (d, 1H, J = 7.2 Hz, $H_{4'}$), 7.07 (t, 1H, J = 7.8 Hz, H_8), 2.69 (dd, 1H, H_β), 2.06 (dd, 1H, $H_{\beta'}$), 1.86 (m, 2H, H_β and $H_{\beta'}$), 1.30 (m, 4H, H_α and $H_{\alpha'}$).

[Cu(4)$_2$]ClO$_4$. Following the procedure described for [Cu(**3a**)$_2$]ClO_4, naphtho[1,2-*b*]-1,10-phenanthroline (**4**, 30 mg, 0.1 mmol) was treated with [Cu(CH_3CN)$_4$]ClO_4 (18 mg, 0.05 mmol) to give [Cu(**4**)$_2$]ClO_4 (33 mg, 92%) as dark green crystals: ^{1}H NMR (CD_3CN) δ 10.12 (d, 2H, $H_{8'}$), 9.16 (s, 2H, H_4), 8.92 (broad s, 2H, H_9), 8.72 (AB quartet, 2H, J = 6.0 Hz, $H_{A'}$), 8.30 (AB quartet, 2H, J = 6.0 Hz, $H_{B'}$), 8.16 (d, 2H, J = 9.0 Hz, H_7), 7.98 (AB quartet, 2H, J = 9.0 Hz, H_5 or H_6), 7.88 (AB quartet, 2H, J = 9.0 Hz, H_5 or H_6), 7.82 (m, 4H, H_8/$H_{3'}$), 7.42 (t, 2H, J = 9.0 Hz, $H_{4'}$), 6.59 (t, 2H, J = 9.0 Hz, $H_{5'}$); MS *m*/*e* 623 (M − ClO_4)$^+$. Anal. Calcd for $C_{40}H_{26}N_4CuClO_4$: C, 66.20; H, 3.58; N, 7.72. Found: C, 66.29; H, 3.27; N, 7.80.

[Cu(5a)$_2$]ClO$_4$. To a solution of 3,3′-dimethylene-2,2′-bibenzo[*h*]-quinoline (**5a**, 20 mg, 0.05 mmol) in $CHCl_3$ (2 mL) was added [Cu(CH_3CN)$_4$]ClO_4 (8.0 mg, 0.02 mmol) in CH_3CN (5 mL). The dark green solution was stirred under Ar at 25 °C for 2 h. Removal of the solvent under vacuum, followed by recrystallization from CH_3CN/toluene (1:1) provided [Cu(**5a**)$_2$]ClO_4 (40 mg, 87%) as green crystals: ^{1}H NMR (CD_3COCD_3) δ 9.37 (d, 2H, J = 8.4 Hz, H_{10}), 8.39 (s, 4H, H_4), 7.52

Table 1. Data Collection and Processing Parameters for $[Cu(\mathbf{4})_2](ClO_4)$ and $[Cu(\mathbf{5c})_2](ClO_4)$

	$[Cu(\mathbf{4})_2](ClO_4)$	$[Cu(\mathbf{5c})_2](ClO_4)$
space group	$P\bar{1}$ (triclinic)	$P\bar{1}$ (triclinic)
cell constants	$a = 11.195(3)$ Å	$a = 11.4871(6)$ Å
	$b = 12.439(3)$	$b = 13.2350(7)$
	$c = 13.072(3)$	$c = 15.6099(8)$
	$\alpha = 69.120(14)°$	$\alpha = 79.749(1)°$
	$\beta = 88.995(14)$	$\beta = 74.663(1)$
	$\gamma = 69.676(13)$	$\gamma = 84.361(1)$
	$V = 1583.2(7)$ Å^3	$V = 2249$ Å^3
molecular formula	$C_{40}H_{24}ClCuN_4O_4$	$C_{60}H_{44}ClCuN_4O_4$
formula weight	723.62	984.07
formula units per cell	$Z = 2$	$Z = 2$
density	$\rho = 1.518$ g-cm^{-3}	$\rho = 1.45$ g-cm^{-3}
absorption coefficient	$\mu = 0.826$ cm^{-1}	$\mu = 6.01$ cm^{-1}
temperature	$T = -50$ °C	$T = -50$ °C
$R_1 = \sum\|\|F_o\| - \|F_c\|\|/\sum\|F_o\|$	0.0385	0.031
$wR_2 = [\sum w(F_o^2 - F_c^2)^2/\sum w(F_o^2)^2]^{1/2}$	0.1030	0.040
weights	$w = [\sigma(F_o^2) + (0.0637P)^2 + (1.805P)]^{-1}$ where $P = (F_o^2 + 2F_c^2)/3$	$w = \sigma(F)^{-2}$

(m, 2H), 7.23 (t, 4H, H_8 or H_9), 6.75 (t, 4H, H_8 or H_9), 3.63 (s, 8H, $-CH_2-$); MS *m/e* 827 $(M)^+$, 445 $(M - L)^+$. Anal. Calcd for $C_{28}H_{18}N_2CuClO_4 \cdot 0.5H_2O$: C, 71.79; H, 3.95; N, 5.98. Found: C, 71.78; H, 3.75; N, 5.98.

$[Cu(\mathbf{5b})_2]ClO_4$. Following the procedure described for $[Cu(\mathbf{5a})_2]ClO_4$, 3,3′-trimethylene-2,2′-bibenzo[*h*]quinoline (**5b**, 40 mg, 0.1 mmol) was treated with $[Cu(CH_3CN)_4]ClO_4$ (16 mg, 0.05 mmol). Removal of the solvent, followed by recrystallization from CH_3CN/toluene (1:1) provided $[Cu(\mathbf{5b})_2]ClO_4$ (80 mg, 83%) as burgundy crystals: ^{1}H NMR (CD_3CN) δ 9.23 (broad s, 2H, $J = 3.0$ Hz, H_{10}), 7.92 (s, 2H, H_4), 7.53 (d, 2H, $J = 7.8$ Hz), 7.42 (AB quartet, 2H, $J = 9.0$ Hz, H_5 or H_6), 7.25 (m, 4H), 6.65 (t, 2H, H_9), 3.12 (m, 4H, $-CH_2-$), 2.91 (t, 4H, $-CH_2-$), 2.44 (t, 4H, $-CH_2-$), MS *m/e* 855 $(M)^+$, 459 $(M - L)^+$. Anal. Calcd for $C_{29}H_{20}N_2CuClO_4$: C, 72.88; H, 4.19; N, 5.86. Found: C, 72.63; H, 4.04; N, 5.79.

$[Cu(\mathbf{5c})_2]ClO_4$. Following the procedure described for $[Cu(\mathbf{5a})_2]ClO_4$, 3,3′-tetramethylene-2,2′-bibenzo[*h*]quinoline (**5c**, 30 mg, 0.07 mmol) was treated with $[Cu(CH_3CN)_4]ClO_4$ (12 mg, 0.04 mmol). Reduction of the solvent under vacuum, followed by cooling overnight, provided $[Cu(\mathbf{5c})_2]ClO_4$ (27 mg, 77%) as bright orange crystals: ^{1}H NMR (CD_3CN) δ 9.23 (broad s, 2H, $J = 3.0$ Hz, H_{10}), 7.92 (s, 2H, H_4), 7.53 (d, 2H, $J = 7.8$ Hz), 7.42 (AB quartet, 2H, $J = 9.0$ Hz, H_5 or H_6), 7.25 (m, 4H), 6.65 (t, 2H, H_9), 3.12 (m, 4H, $-CH_2-$), 2.91 (t, 4H, $-CH_2-$), 2.44 (t, 4H, $-CH_2-$), MS *m/e* 883 $(M - ClO_4)^+$, 473 $(M - L)^+$. The analogous hexafluorophosphate salt was also prepared (54%). Anal. Calcd for $C_{60}H_{44}N_4CuPF_6$: C, 70.00; H, 4.28; N, 5.44. Found: C, 69.81; H, 4.55; N, 5.34.

Spectroscopy. NMR spectra were recorded on a General Electric QE−300 Spectrometer at 300 MHz for ^{1}H and 75 MHz for ^{13}C. Chemical shifts are reported in parts per million downfield from internal TMS with solvent peaks as reference. Absorption spectra were measured on a Perkin-Elmer Lambda 3B or a Hewlett-Packard 8453 diode array spectrophotometer. Photoluminescence spectra were run on either on a Perkin-Elmer LS-50 or Spex Fluorolog II fluorimeter. The SPEX Fluorolog was corrected for spectral response using a calibrated lamp. Photoluminescence quantum yield measurements were performed using the optically dilute technique[17] with $[Ru(bpy)_3](Cl)_2$ in deionized H_2O ($\Phi_{em} = 0.042$) as the actinometer. Time-resolved photoluminescence decays were acquired and analyzed on an apparatus that has been previously described.[18] Time-resolved absorption measurements were carried out as previously described.[19] Mass spectra were obtained on a Hewlett-Packard 5989B mass spectrometer (59987A electrospray) using atmospheric pressure ionization at 160 °C for the complexes and atmospheric pressure chemical ionization at 300 °C for the ligands.

X-ray Determinations. $[Cu(\mathbf{5c})_2](ClO_4)$. A red fragment having approximate dimensions 0.20 × 0.35 × 0.40 mm was cut from a large multifaceted block and mounted in a random orientation on a Siemens SMART platform diffractometer equipped with a 1K CCD area detector. The sample was placed in a stream of dry nitrogen gas at −50 °C, and the radiation used was Mo Kα monochromatized by a highly ordered graphite crystal. A hemisphere of data (1271 frames at 5 cm detector distance) was collected using a narrow-frame method with scan widths of 0.30° in omega and an exposure time of 15 s/frame. The first 50 frames were remeasured at the end of data collection to monitor instrument and crystal stability, and the maximum correction on *I* was <1%. The data were integrated using the Siemens SAINT program, with the intensities corrected for Lorentz factor, polarization, air absorption, and detector faceplate. A psi scan absorption correction was applied based on the entire data set. Redundant reflections were averaged. Final cell constants were refined using 8027 reflections having $I > 10\sigma(I)$, and these, along with other information pertinent to data collection and refinement, are listed in Table 1. The Laue symmetry was determined to be 1(bar), and the space group was shown to be either $P1$ or $P\bar{1}$.

Since the unitary structure factors displayed centric statistics, space group $P\bar{1}$ was assumed from the outset. The structure was solved by interpretation of the Patterson map, which revealed the position of the Cu atom. Remaining non-hydrogen atoms were located in subsequent difference Fourier syntheses. The usual sequence of isotropic and anisotropic refinement was followed, after which all of the hydrogens were entered in ideal calculated positions and constrained to riding motion, with a single variable isotropic thermal parameter for all of them. After all shift/esd ratios were less than 0.1 convergence was reached at the agreement factors listed in Table 1. No unusually high correlations were noted between any of the variables in the last cycle of full-matrix least squares refinement, and the final difference density map showed a maximum peak of about 0.3 e/Å^3. All calculations were made using Nicolet's SHELXTL PLUS (1987) series of crystallographic programs.[20]

$[Cu(\mathbf{4})_2](ClO_4)$. A reddish-brown flat column having approximate dimensions 0.55 × 0.20 × 0.15 mm was mounted in a random orientation on a Nicolet R3m/V automatic diffractometer in a stream of dry nitrogen gas at −50 °C. The radiation used was Mo Kα monochromatized by a highly ordered graphite crystal. Final cell constants, as well as other information pertinent to data collection and refinement, are listed in Table 1. The Laue symmetry was determined to be −1, and the space group was shown to be either $P1$ or $P\bar{1}$. Intensities were measured using the Θ:2Θ scan technique, with the scan rate depending on the count obtained in rapid pre-scans of each reflection. Three standard reflections were monitored after every 2 h

(17) Demas, J. N.; Crosby, G. A. *J. Phys. Chem.* **1971**, *75*, 991.
(18) Castellano, F. N.; Heimer, T. A.; Tandhasetti, T.; Meyer, G. J. *Chem. Mater*. **1994**, *6*, 1041.
(19) Ruthkosky, M.; Castellano, F. N.; Meyer, G. J. *Inorg. Chem*. **1996**, *35*, 6406.
(20) Sheldrick, G. M. In *Crystallographic Computing 3*; Sheldrick, G. M., Kruger, C., Goddard, R., Eds.; Oxford University Press: Oxford, U. K., 1985; pp 175−189.

or every 97 data collected, and these showed no significant change over the course of the experiment. During data reduction Lorentz and polarization corrections were applied as well as empirical absorption correction based on psi scans of 10 reflections having chi values near 90°.

The unitary structure factors displayed centric statistics, and so space group $P\bar{1}$ was assumed from the outset. The structure was solved by interpretation of the Patterson map, which revealed the position of the Cu atom. Remaining nonhydrogen atoms were located in subsequent difference Fourier syntheses. The usual sequence of isotropic and anisotropic refinement was followed, after which all hydrogens were entered in ideal calculated positions and constrained to riding motion, with a single variable isotropic temperature factor for all of them. After all shift/esd ratios were less than 0.1 convergence was reached at the agreement factors listed in Table 1. No unusually high correlations were noted between any of the variables in the last cycle of full-matrix least-squares refinement, and the final difference density map showed a maximum peak of about 0.77 e/A^3. All calculations were made using the SHELXS-97 series of crystallographic programs.[20]

Results and Discussion

Synthesis and Characterization. Both series of ligands were synthesized in a single step, involving the Friedländer condensation of 1-amino-2-naphthaldehyde (**7**) with an appropriate ketone or diketone.[15] For the series **3a**−**c**, 2-acetylpyridine (**6a**) and the previously reported pyridyl ketones (**6b**−**d**)[13] were employed as the carbonyl component and yields varied from 71% to 77%. The dimethylene bridged system **3b** could be dehydrogenated by treatment with palladium on charcoal in refluxing nitrobenzene to give a 46% yield of the fully aromatized material **4**.[14] The 2,2′-bibenzo[*h*]quinolines **5a**−**c** were prepared in yields of 37−74% by the 2:1 condensation of **7** with the 1,2-cycloalkanediones **8a**−**c**. In several cases, improved yields resulted from carrying out the condensation in refluxing toluene under Dean−Stark conditions where water could be azeotropically removed from the reaction mixture. The yield of **5a** was improved by using piperidine instead of KOH as the catalyst. The model compound **9** was prepared in a similar manner from cyclohexanone.

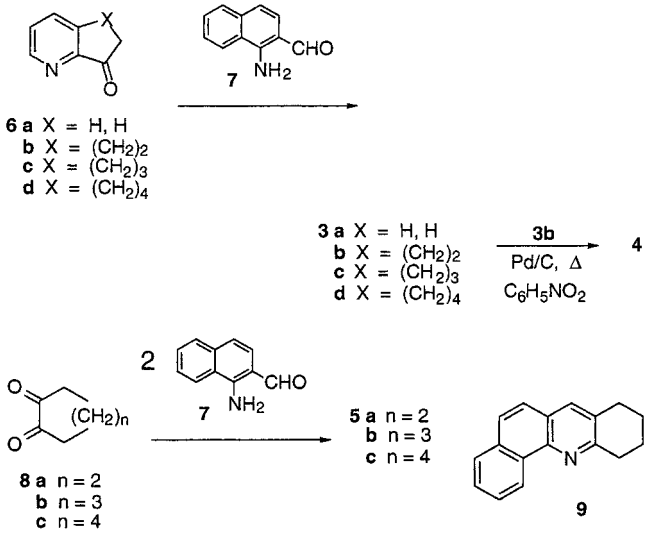

Treating the ligands with 0.5 equiv of $[Cu(CH_3CN)_4]ClO_4$ in acetonitrile at room temperature under argon afforded the Cu(I) complexes. Upon addition of the Cu(I) reagent, the clear ligand solution immediately became deeply colored and the complex was isolated by concentration. In the case of **5a**−**c**, the ligand was first dissolved in a small amount of $CHCl_3$. The corresponding hexafluorophosphate salts could be prepared by using $[Cu(CH_3CN)_4]PF_6$ in a similar manner. All new complexes gave the expected base peak in their electrospray mass spectra and exhibited correct elemental analyses.

Table 2. Selected ^{1}H NMR Data[a] for 2-(2′-Pyridyl)-benzo[*h*]-quinolines,[b] 2,2′-Bibenzo[*h*]quinolines[c] and Their Cu(I) Complexes

ligand/complex	H_4	CIS	H_9	CIS	H_{10}	CIS
3a	8.38		7.77		9.42	
3b	8.12		7.75		9.35	
3c	8.19		7.74		9.24	
3d	8.24		7.74		9.12	
4	8.90		7.76		9.20	
$[Cu(\mathbf{3a})_2]ClO_4$	7.90	+0.48	6.85	+0.92	8.72	+0.70
$[Cu(\mathbf{3b})_2]ClO_4$	7.79	+0.33	6.81	+0.94	8.83	+0.52
$[Cu(\mathbf{3c})_2]ClO_4$	7.42	+0.77	7.02	+0.72	8.82	+0.42
$[Cu(\mathbf{3d})_2]ClO_4$	7.40	+0.84	7.45	+0.29	8.83	+0.29
$[Cu(\mathbf{4})_2]ClO_4$	9.16	-0.26	7.82	-0.06	8.92	+0.28
5a	8.28		7.75		9.77	
5b	8.22		7.65		9.38	
5c	8.35		7.70		9.28	
9	7.80		*d*		9.28	
$[Cu(\mathbf{5a})_2]ClO_4$	8.39	-0.11	6.75	+1.00	9.37	+0.40
$[Cu(\mathbf{5b})_2]ClO_4$	8.14	+0.08	6.88	+0.77	9.35	+0.03
$[Cu(\mathbf{5c})_2]ClO_4$	8.06	+0.29	6.95	+0.75	9.34	+0.06

[a] Measured at 25 °C and reported in ppm referenced to TMS; CIS = coordination induced shift. [b] Ligands and complexes measured in CD_3CN. [c] Ligands and complexes measured in CD_3COCD_3. [d] Could not be assigned due to overlapping signals.

^{1}H NMR Properties. Both ligands and complexes could be readily characterized by their ^{1}H NMR spectra. For the naphtho-[1,2-*b*]pyridine ring, the H4 proton appeared as a singlet; the H5 and H6 protons appeared as an AB quartet; and the terminal benzo-ring gave a characteristic pattern with the proton closest to the bay region being strongly deshielded and thus shifted to below 9 ppm. For the symmetrical 2,2′-bibenzo[*h*]quinolines **5a**−**c**, the bridge protons appeared as a singlet for the dimethylene-bridged system **5a** and a downfield triplet (4H) and upfield quintet (2H) for the trimethylene-bridged system **5b**, indicating that conformational inversion by twisting about the 2,2′-bond was rapid on the NMR time scale.[21] For the tetramethylene bridged derivative **5c**, this conformational inversion was sufficiently slow that, at room temperature, four nonequivalent two-proton signals were observed in the upfield region.

Analysis of the ^{1}H NMR data given in Table 2 shows shielding and deshielding effects for the free ligands that are consistent with conformational variations in these systems associated with the length of the 3,3′-bridge. For each series of bridged ligands, H4 appears in a narrow range and is relatively insensitive to conformation but is shifted about 0.4 ppm downfield compared to the model compound **9**, apparently due to increased delocalization. On the other hand, H10, being held closest to the bay region is quite sensitive to conformation and is most deshielded, appearing at 9.77 ppm for the more planar **5a** and shifting up to 9.28 ppm for the highly twisted **5c**, which corresponds exactly to the value for the model **9**. As expected, somewhat less pronounced, but similar, shielding effects are observed for H10 in the series **3a**−**d**. For the free ligands, H9 also falls into a more narrow range, 7.74−7.77 ppm for **3a**−**d** and 6.75−6.95 ppm for **5a**−**c**.

For the Cu(I) complexes, tetrahedral coordination would normally require that the two ligands be situated in approximately orthogonal planes. However, the nonplanarity of the ligand, dictated by the 3,3′-polymethylene bridge, causes

(21) (a) Thummel, R. P.; Lefoulon, F.; Mahadevan, R. *J. Org. Chem.* **1985**, *50*, 3824. (b) Thummel, R. P.; Lefoulon, F. *J. Org. Chem.* **1985**, *50*, 666.

Table 3. Calculated Geometric Features for Energy Minimized Structures of 2,2′-Bibenzo[*h*]quinolines, and Their Cu(I) Complexes[a]

compound	$N_1-C-C-N_{1'}$[b] (deg)	$N_1-N_{1'}$ (Å)
5a	16	3.08
5b	44	3.14
5c	61	3.22
$[Cu(\mathbf{5a})_2]^+$	16	2.86
$[Cu(\mathbf{5b})_2]^+$	31	2.84
$[Cu(\mathbf{5c})_2]^+$	37	2.83

[a] Calculated using PC MODEL from Serena Software, Bloomington, IN. [b] Average of $N_1-C_2-C_{2'}-N_{1'}$ and $C_3-C_2-C_{2'}-C_{3'}$.

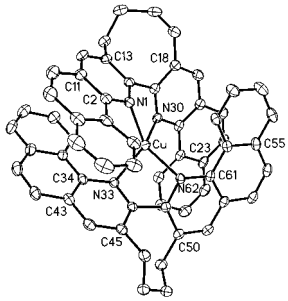

Figure 1. ORTEP diagram of the cation of $[Cu(\mathbf{5c})_2](ClO_4)$ with atomic numbering for key atoms.

these ligands to adopt a more helical shape in the coordination sphere. From Table 2 we observe that, with only two small exceptions, the protons H4, H9, and H10 all shift upfield upon coordination. This shift can be attributed to a tendency for the benzo[*h*]quinoline (BHQ) rings on the opposing ligands to align themselves in a parallel π-stacked array. The longer the polymethylene bridge, the more able the ligand is to accommodate this distortion. The result is that H4 experiences increased shielding along the series $[Cu(\mathbf{3a}-\mathbf{d})_2]^+$ and $[Cu(\mathbf{5a}-\mathbf{c})_2]^+$ as it finds itself closer to the opposing ligand with increasing bridge length.

The protons H9 and H10, which are closer to the bay region of the free ligand, are consequently pointed more toward the orthogonal ligand in the Cu(I) complex. This orientation causes a fairly strong shielding effect. For the complexes of **3a**−**d**, H9 moves upfield from 0.29 to 0.92 ppm. The effect is somewwhat diminished for H10 which is upfield shifted from 0.29 to 0.70 ppm. The shifts are greatest for the more planar unbridged and dimethylene bridged systems where π-stacking is less important. For the more crowded series **5a**−**c**, the same effects are evidenced with H9 again being more affected than H10.

Structural Analysis. Molecular mechanics calculations were carried out to simulate the minimum energy geometries of **5a**−**c** and $[Cu(\mathbf{5a}-\mathbf{c})_2]^+$ and to analyze the conformational effects of bridging. A few pertinent aspects of these calculations are summarized in Table 3. For the free ligands the dihedral angle between the BHQ rings increases from 16° for the dimethylene-bridged system to 61° for the tetramethylene-bridged system. The corresponding distance between the two nitrogens increases from 3.08 to about 3.22 Å. Complexation is expected to cause the ligands to "flatten" and the dihedral angles decrease to 31° and 37° for the complexes of **5b**,**c** respectively. This flattening is predicted to keep the N−N distance almost invariant.

We have recently reported the structure of $[Cu(\mathbf{2d})_2]^+$ where the highly twisted ligand led to an unusually distorted complex.[5] It was expected that the benzo[*h*]-fusion in **5c** would cause even greater congestion and perhaps more pronounced distortion. Figure 1 shows an ORTEP drawing of the cation of $[Cu(\mathbf{5c})_2](ClO_4)$ and Figure 2 shows comparable views which emphasize

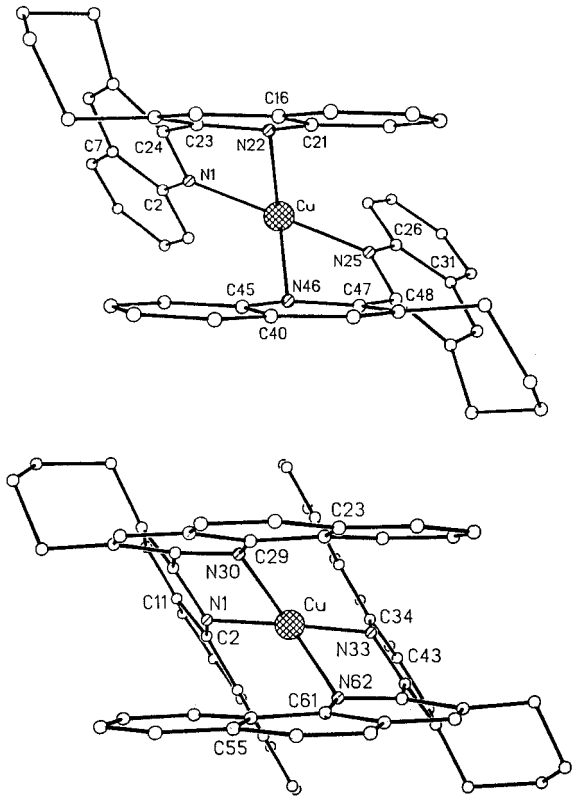

Figure 2. Comparison of the structures for the cation of $[Cu(\mathbf{2d})_2](ClO_4)$ (top) and $[Cu(\mathbf{5c})_2](ClO_4)$ (bottom).

π-stacking for this cation and the analogous complex of **2d**. Table 4 compares selected geometric properties for both complexes and it is apparent that, although $[Cu(\mathbf{5c})_2]^+$ is more congested, it is actually less distorted. The Cu−N bond lengths are all similar, 2.07−2.08 Å, and just slightly longer than other typical Cu(I) phen complexes (2.02−2.07 Å).[22] For the complex of **2d** there was a great disparity of Cu−N distances falling outside the normal range. The 2,2′-bond connecting the two halves of ligand **5a** is 1.49 Å, essentially the same as the complex of **2d.** The N−Cu−N bond angles involving a unique ligand are 84°, which is somewhat larger than the 80−81° observed for other Cu(I) phen systems. This is understandable in light of the increased dihedral angle between the two benzo-[*h*]quinoline halves of the ligand, about 48°, as opposed to 42° for $[Cu(\mathbf{2d})_2]^+$. The measured value of 48° is considerably greater than the 37° estimated for the energy minimized structure (Table 3) which probably reflects the inability of the modeling program to deal with $\pi-\pi$ interactions. The four other N−Cu−N angles given in Table 4 indicate the degree to which the mean planes of the two ligands vary from the orthogonal array of an ideal tetrahedron wherein all four N−Cu−N angles would be equal at about 109°. The variation between approximately 111° and 138° shows some twisting about the metal center but still a more organized geometry than what was observed for $[Cu(\mathbf{2d})_2]^+$, where the angles vary from 93° to 152°.

The most striking observation is that the BHQ moieties of opposing ligands are aligned almost parrallel to one another so that their mean planes intersect with an angle of about 8.5°.

(22) (a) Healy, P. C.; Engelhardt, L. M.; Patrick, V. A.; White, A. H. *J. Chem. Soc., Dalton Trans.* **1985**, 2541. (b) Klemens, F. K.; Fanwick, P. E.; Bibler, J. K.; McMillin, D. R. *Inorg. Chem.* **1989**, *28*, 3076. (c) Geoffroy, M.; Wermeille, M.; Buchecker, C. O.; Sauvage, J.-P.; Bernardinelli, G. *Inorg. Chim. Acta* **1990**, *167*, 157.

Table 4. Selected Bond Lengths, Bond Angles, and Dihedral Angles for $[Cu(\mathbf{2d})_2](BF_4)$, $[Cu(\mathbf{5c})_2](ClO_4)$, and $[Cu(\mathbf{4})_2](ClO_4)$[a]

$[Cu(\mathbf{2d})_2](BF_4)$[4]		$[Cu(\mathbf{5c})_2](ClO_4)$		$[Cu(\mathbf{4})_2](ClO_4)$	
		Bond Lengths (Å)			
Cu−N1	1.979(2)	Cu−N1	2.067(2)	Cu−N1	2.005(3)
Cu−N22	2.225(2)	Cu−N30	2.077(2)	Cu−N20	2.136(3)
Cu−N25	1.984(2)	Cu−N33	2.068(2)	Cu−N23	2.003(3)
Cu−N46	2.189(3)	Cu−N62	2.076(2)	Cu−N42	2.127(3)
C23−C24	1.492(4)	C31−C32	1.487(3)	C21−C22	1.446(5)
C47−C48	1.493(3)	C63−64	1.489(3)	C18−C19	1.448(6)
		Bond Angles (deg)			
N1−Cu−N22	80.0(1)	N1−Cu−N30	84.1(1)	N1−Cu−N20	81.80(11)
N25−Cu−N46	80.4(1)	N33−Cu−N62	83.9(1)	N23−Cu−N42	82.28(10)
N1−Cu−N25	152.1(1)	N1−Cu−N33	111.7(1)	N1−Cu−N23	118.07(11)
N22−Cu−N46	93.5(1)	N30−Cu−N62	110.1(1)	N20−Cu−N42	110.53(10)
N1−Cu−N46	120.3(1)	N1−Cu−N62	136.3(1)	N1−Cu−N42	137.46(11)
N22−Cu−N25	119.8(1)	N30−Cu−N33	140.3(1)	N20−Cu−N23	135.42(11)
		Dihedral Angles (deg)			
N22−C23−C24−N1	43.6	N30−C31−C32−N1	47.9	N20−C21−C22−N1	6.2(5)
N46−C47−C48−N25	40.9	N62−C63−C64−N33	48.3	N42−C43−C44−N23	3.6(4)
C40−C45−N46−Cu	127.0	C52−C61−N62−Cu	133.2	C17−C18−C19−N20	5.9(5)
C16−C21−N22−Cu	124.3	C20−C29−N30−Cu	133.8	C39−C40−C41−N42	4.9(5)
C31−C26−N25−Cu	167.0	C43−C34−N33−Cu	135.4	C5−C22−N1−Cu	171.5(3)
C7−C2−N1−Cu	162.9	C11−C2−N1−Cu	136.1	C8−C21−N20−Cu	163.9(3)
				C27−C44−N23−Cu	171.4(2)
				C30−C43−N42−Cu	168.3(2)

[a] Numbering pattern from Figures 1 and 3 with esd's in parentheses.

The approximate distance between these mean planes is 3.36−3.38 Å which is very close to the distance of 3.35 Å which occurs between the two parallel quinoline rings in $[Cu(\mathbf{2d})_2]^+$.[5] Since **5c** is just a dibenzo-fused analogue of **2d**, it appears that this additional π-surface, rather than causing further distortion, actually increases the $\pi-\pi$ attraction and allows the complex to assume a more organized geometry. This arrangement comes at the expense of optimal overlap of the nitrogen lone pair electrons and the Cu(I) d-orbitals. This alignment can be evaluated by looking at the C_a-C_b-N-Cu dihedral angle where C_a and C_b denote the two central fused carbons of the quinoline ring. In a tetrahedral Cu(I) complex where the two ligands are perfectly orthogonal, this angle should be 180°. For $[Cu(\mathbf{5c})_2]^+$ these angles measure 133−136°, indicating a considerable distortion of the coordinative bond but a fairly high degree of symmetry. Note that the two parallel quinoline rings in $[Cu(\mathbf{2d})_2]^+$ are even less well aligned with an average angle of about 126°.

It became of interest to examine the structure of the copper complex of the fully aromatized naphthophen **4**. When compared to **3a**−**d** or **5a**−**c**, this ligand is unique in two respects. First, it has a large π-surface, consisting of five fused aromatic rings. Hence one might expect π-stacking effects to be important. Second, the two ligating pyridine rings of each ligand are held essentially coplanar, being part of a phen subunit. The possibility for helical distortions, as is found in the bridged ligands, is thus greatly diminished.

Figure 3 shows an ORTEP plot of the cation of $[Cu(\mathbf{4})_2]^+$ and pertinent geometric features are summarized in Table 4. The complex is distorted from tetrahedral geometry to allow the BHQ subunits to approach one another as closely as possible. One result is a disparity in the Cu−N bond lengths much like what was observed in $[Cu(\mathbf{2d})_2]^+$. The exterior pyridine rings (N1 and N23) form bonds of about 2.00 Å while the interior pyridine rings form Cu−N bonds of 2.13−2.14 Å. As expected, the bond joining the two pyridines is now shorter (1.45 Å) as it is contained in an aromatic ring. The intraligand N−Cu−N angles are somewhat diminished as compared to $[Cu(\mathbf{5c})_2]^+$ due to congestion around the metal. The interligand N−Cu−N angles are rather similar to $[Cu(\mathbf{5c})_2]^+$ indicating some symmetry

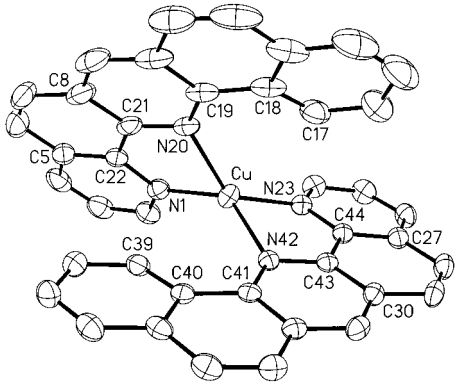

Figure 3. ORTEP diagram of the cation of $[Cu(\mathbf{4})_2](ClO_4)$ with atomic numbering for key atoms.

but also considerable distortion. The inability of the BHQ rings to π-stack as effectively as they do for the complexes of **2d** and **5c** is reflected by better alignment of the nitrogen lone pair electrons and the Cu(I) d-orbitals. The C_a-C_b-N-Cu angles are much closer to the ideal 180° than was found in the other two complexes.

Electrochemical Properties. The redox properties of the copper complexes were evaluated in dichloromethane and acetonitrile electrolyte solutions. In all cases, quasi-reversible waves were observed and reasonably assigned to the Cu(I/II) couple and the half-wave oxidation potentials are reported in Table 5. It is interesting to note that the two systems $[Cu(\mathbf{3a})_2]^+$ and $[Cu(\mathbf{3d})_2]^+$ for which we were unable to observe an oxidative wave are also the ones which do not exhibit a clear MLCT absorption band. Oxidation of Cu(I) to Cu(II) is associated with a geometric flattening of the molecule from pseudo-tetrahedral to square planar or square pyramidal. Substituents in the 2,9-positions of phen ligands tend to sterically impede this process leading to more positive oxidation potentials. The ligands **3a**−**d** are composed of a 2,2′-bonded pyridine and BHQ ring which provides steric impediment to only one-half of such a ligand. Thus oxidative flattening which forces the two pyridine rings away from each other is not particularly unfavorable and potentials of 0.58 and 0.62 V are measured

Table 5. Half-Wave Potentials for Benzo[*h*]quinoline Cu(I) Complexes[a]

	$E_{1/2}$	
complex	CH_3CN	CH_2Cl_2
$[Cu(\mathbf{3a})_2]^+$	no wave observed	
$[Cu(\mathbf{3b})_2]^+$	+0.58 (60)	
$[Cu(\mathbf{3c})_2]^+$	+0.62 (90)	
$[Cu(\mathbf{3d})_2]^+$	no wave observed	
$[Cu(\mathbf{4})_2]^+$	+0.62 (70)	
$[Cu(\mathbf{5a})_2]^+$		+0.99 (60)
$[Cu(\mathbf{5b})_2]^+$		+1.12 (64)
$[Cu(\mathbf{5c})_2]^+$		+1.17 (62)

[a] Potentials are in volts vs SCE; solutions were 0.1M TBAP in CH_3CN or CH_2Cl_2; $T = 25 \pm 1$ °C; the sweep rate was 200 mV/s; the number in parentheses is the difference (mV) between the anodic and cathodic waves.

Table 6. Electronic Absorption Data for 2-(2′-Pyridyl)-benzo[*h*]-quinolines, 2,2′-Bibenzo[*h*]quinolines, and Their Cu(I) Complexes

compound[a]	λ_{max} (ϵ)[b]
3a	238 (46,140), 287 (24,830), 311 (13,170), 357 (9,270)
3b	245 (51,980), 299 (24,040), 347 (13,570), 364 (17,520)
3c	243 (49,246), 279 (26,160), 335 (6,480), 351 (7,170)
3d	244 (52,000), 273 (37,600), 333 (6,200), 350 (6,900)
4	240 (28,520), 294 (56,240), 349 (6,440) 366 (5,370), 387 (5,740)
$[Cu(\mathbf{3a})_2]^+$	237 (77,240), 287 (49,520), 311 (26,600), 340 (18,060), 357 (20,314)
$[Cu(\mathbf{3b})_2]^+$	243 (78,270), 300 (35,140), 347 (18,820), 364 (24,890), 549 (850)
$[Cu(\mathbf{3c})_2]^+$	241 (86,780), 279 (44,780), 335 (12,360), 351 (13,350), 500 (s, 510)
$[Cu(\mathbf{3d})_2]^+$	241 (100,000), 273 (80,800), 333 (15,600), 350 (17,500)
$[Cu(\mathbf{4})_2]^+$	293 (84,290), 304 (65,200), 348 (12,160), 366 (10,470), 451 (1,700)
5a	238 (70,300), 297 (29,420), 367 (18,140), 385 (31,280)
5b	237 (72,250), 284 (29,160), 338 (12,270), 356 (15,480), 385 (1,800)
5c	237 (68,370), 275 (41,030), 319 (7,660), 334 (10,640), 351 (12,150)
9	242 (37,370), 269 (21,880), 318 (1,350), 333 (4.080), 349 (5,030)
$[Cu(\mathbf{5a})_2]^+$	308 (48,940), 393 (32,690), 413 (29,080), 610 (1,850)
$[Cu(\mathbf{5b})_2]^+$	304 (48,300), 326 (22,640), 376 (26,200), 539 (1,960)
$[Cu(\mathbf{5c})_2]^+$	301 (48,760), 326 (19,940), 373 (20,520), 496 (1,850)

[a] 5×10^{-5} M in CH_3CN at 25 °C. [b] Wavelength reported in nm.

for $[Cu(\mathbf{3b},\mathbf{c})_2]^+$. When both halves of the ligand are bulky BHQs, a favorable flattening route is no longer available and the oxidation potentials for $[Cu(\mathbf{5a}\text{-}\mathbf{c})_2]^+$ increase accordingly to +0.99−1.12 V.

Photophysical Properties. The electronic absorption data of **3a**−**d**, **4**, **5a**−**c**, and **9** and their Cu(I) complexes are summarized in Table 6. The ligands show an absorption maximum which increases in energy and decreases in intensity as the length of the 3,3′-polymethylene bridge increases. This trend is consistent with a decrease in the electronic interaction between the two halves of the molecule as the dihedral angle between them increases. The profile for **5c** is nearly identical to **9** indicating that for this system there is very little electronic communication between the two benzo[*h*]quinolines. As expected, the molar absorptivities for **5c** are approximately double those of the model compound.

The copper complexes, $[Cu(\mathbf{5a}\text{-}\mathbf{c})_2]^+$, show ligand based absorptions in the UV, and a less intense MLCT band in the visible region. A 114 nm (3800 cm^{-1}) shift in the MLCT absorption is observed and the color of the dissolved complexes varies from green to purple to orange as the length of the 3,3′-polymethylene chain increases. Interestingly, the molar extinction coefficients of the visible bands are chain length independent. Light excitation into the visible bands results in room-temperature photoluminescence, PL, for complexes $[Cu(\mathbf{5a}-\mathbf{c})_2]^+$ in CH_2Cl_2 (Figure 4) and for $[Cu(\mathbf{5a}-\mathbf{b})_2]^+$ in CH_3CN. Copper complexes with the asymmetric ligands, $[Cu(\mathbf{3a}-\mathbf{d})_2]^+$ and $[Cu(\mathbf{4})_2]^+$, were nonemissive under these conditions. The PL properties of $[Cu(\mathbf{5a}-\mathbf{c})_2]^{+}$* also show systematic trends in the color of the emitted light, the excited-state lifetime, τ, and the quantum yield. The 5.3 μs lifetime and 0.10 quantum yield for $[Cu(\mathbf{5c})_2]^+$ are the highest ever reported for a copper diimine excited state. The relevant energy gap for MLCT transitions is the energy separation between the ligand π*-orbitals and the Cu(I/II) potential. Since the Cu(I/II) oxidation potentials change relatively little with chain length, the spectroscopic data indicates that the π*-levels decrease in a regular fashion over the series $[Cu(\mathbf{5a}-\mathbf{c})_2]^+$, much like the free ligands.

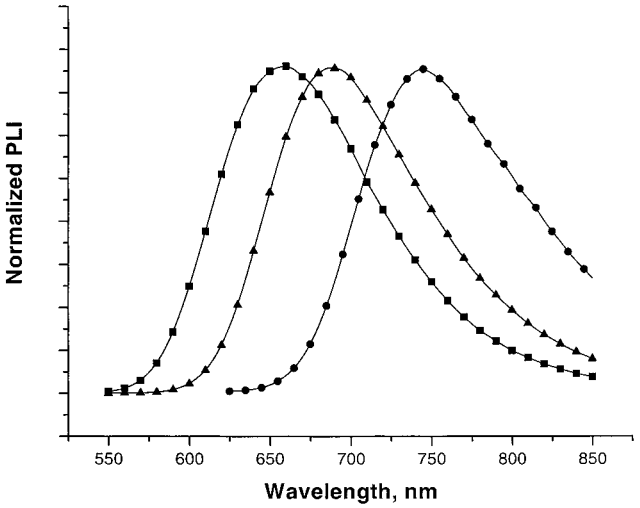

Figure 4. Normalized steady-state photoluminescence spectra of $[Cu(\mathbf{5a})_2]^+$ (circles), $[Cu(\mathbf{5b})_2]^+$ (triangles) $[Cu(\mathbf{5c})_2]^+$ (squares) measured in CH_2Cl_2 at room temperature.

The copper complexes, $[Cu(\mathbf{5a}-\mathbf{c})_2]^+$, displayed long-lived absorption transients after being pulsed with 532.5 nm light excitation in CH_2Cl_2 (Figure 5). The difference spectra are typical of MLCT excited states with positive absorptions from the reduced BHQ ligands, clean isosbestic points, and a negative feature at long wavelengths due to emission. The kinetics are first-order with lifetimes that are, within experimental error, the same as those measured by time-resolved PL, indicating that the time-resolved absorption and PL are probing the same MLCT state. The first-order kinetic rate constants were independent of the irradiance (0.8−10 mJ/pulse), the solution concentration (0.08−0.29 mM), and the monitoring wavelength. The nonemissive copper complexes displayed instrument response limited transients consistent with short excited-state lifetimes, $\tau < 10$ ns.

The experimentally measured τ and Φ values were used to calculate the radiative, k_r, and the nonradiative, k_{nr}, rate constants using standard equations and assuming an intersystem crossing yield of unity (Table 7).[23] The k_r values of $\sim 10^3-10^4$ s^{-1} are typical of copper MLCT excited states. Nonradiative decay for $[Cu(\mathbf{3a}-\mathbf{d})_2]^{+}$* and $[Cu(\mathbf{4})_2]^{+}$* is rapid, $k_{nr} > 10^8$ s^{-1}. The k_{nr} values for $[Cu(\mathbf{5a}-\mathbf{c})_2]^{+}$* are remarkable for copper and over an order of magnitude slower than those typically reported for copper phen excited states. This slow nonradiative decay accounts for the unusually long excited-state lifetimes of these complexes, a point that will be elaborated below.

(23) Murov, S. L.; Carmichael, I.; Hug, G. L. *Handbook of Photochemistry*, 2nd ed.; Marcel Dekker: New York, 1993.

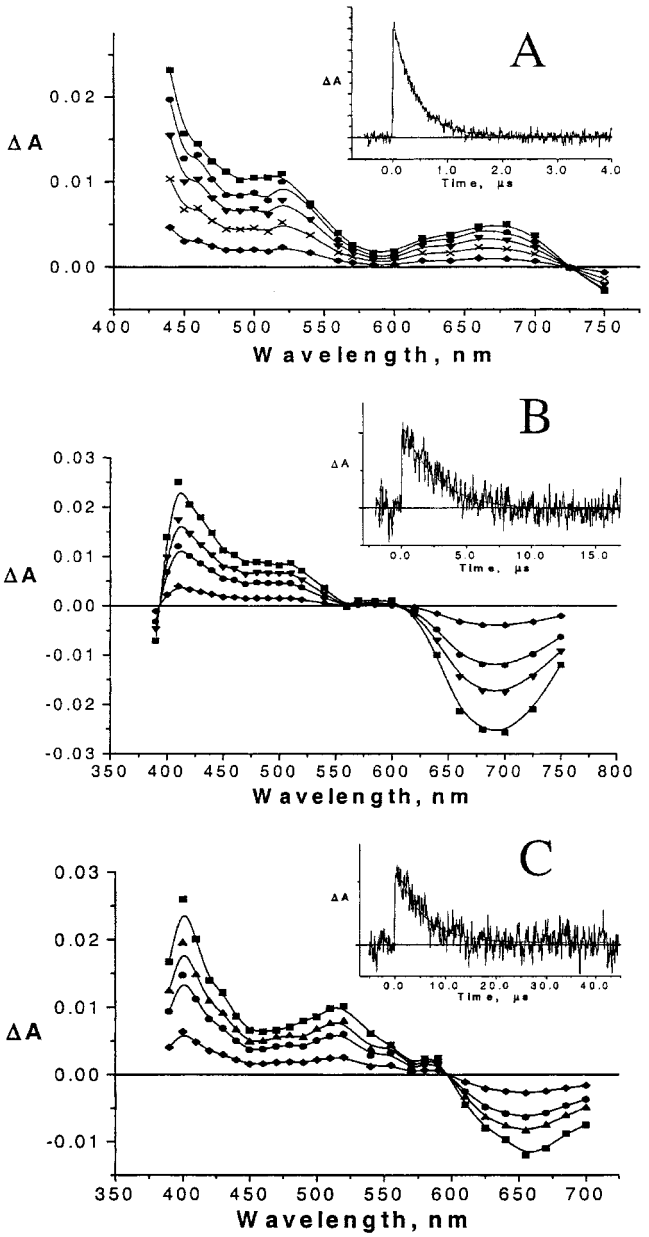

Figure 5. Absorption difference spectra recorded in CH_2Cl_2 at 25 °C after pulsed 532.5 nm light excitation and uncorrected for photoluminescence. (A) $[Cu(\mathbf{5a})_2]^+$ measured at delay times of 0 ns (squares), 100 ns (circles), 250 ns (down triangles), 500 ns (crosses), and 1 μs (diamonds); (B) $[Cu(\mathbf{5b})_2]^+$ measured at delay times of 0 ns (squares), 500 ns (down triangles), 1 μs (circles), and 5 μs (diamonds); and (C) $[Cu(\mathbf{5c})_2]^+$ measured at delay times of 0 ns (squares), 1 μs (up triangles), 5 μs (circles), and 10 μs (diamonds). The inset in each panel shows a single wavelength absorption transient measured at 450 nm with a superimposed fit (solid line) to a first-order kinetic model.

Table 7. Photoluminescence Data for the Complexes $[Cu(\mathbf{5a}-\mathbf{c})_2]^+$ in CH_2Cl_2 and CH_3CN

complex	λ_{max}, nm	τ, μs	$\Phi \times 10^2$	k_r, s^{-1}	k_{nr}, s^{-1}
			CH_2Cl_2		
$[Cu(\mathbf{5a})_2](PF_6)$	720	0.63	0.55	8.8×10^3	1.59×10^6
$[Cu(\mathbf{5b})_2](PF_6)$	670	2.50	4.30	1.7×10^4	3.8×10^5
$[Cu(\mathbf{5c})_2](PF_6)$	660	5.0	10.50	2.1×10^4	1.8×10^5
			CH_3CN		
$[Cu(\mathbf{5a})_2](PF_6)$	740	0.42	0.17	3.9×10^3	2.39×10^6
$[Cu(\mathbf{5b})_2](PF_6)$	680	1.67	1.90	1.1×10^4	5.9×10^5

To better understand the excited-state behavior of these copper compounds, it is worthwhile to consider the intriguing photophysical properties of the well studied bis-phen copper complexes.[2] Bulky alkyl or aryl substituents in the 2- and 9-positions of phen stabilize the Cu(I) geometry by enforcing a tetrahedral, T_d, geometry that inhibits the "flattened" square planar, SP, geometry preferred in the Cu(II) state. Yet, this same flattening is present in the formally Cu(II) MLCT excited state. Karpishin has noted that two geometric features are important for the creation of long-lived excited states: bulky substituents in the 2,9-positions and distortion of the tetrahedral geometry due to interligand interactions.[4] Therefore, an intriguing dichotomy appears to exist in ligand design for long-lived copper MLCT excited states: bulky substituents are required to enforce a tetrahedral geometry while, at the same time, interligand interactions are needed to distort the geometry away from tetrahedral.

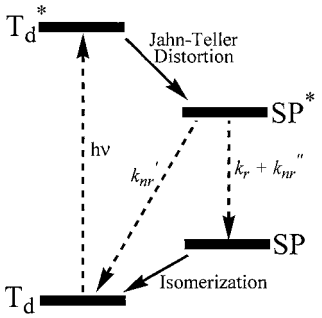

Figure 6. A simplified four level model to describe the absorption and emissive states of copper diimine compounds where a tetrahedral, T_d, Cu(I) and a square planar, SP, Cu(II) geometry is assumed.

This dichotomy can be better understood with the aid of a four-level model that shows the states involved in light absorption and emission (Figure 6).[24] The model applies to any fluorophore with different geometries for the absorbing and emitting states, however for clarity we assume a T_d Cu(I) geometry and a SP Cu(II) geometry as limiting cases. Absorption of a photon promotes an electron from the Cu *d*-orbitals to the π^*-orbitals of the diimine ligand, $d^{10}\pi^{*0} \rightarrow d^9\pi^{*1}$. The excited state initially created is tetrahedral, labeled T_d*, but rapid vibrational relaxation and a significant Jahn−Teller distortion are expected.[25] This inner-sphere reorganization yields a thermally equilibrated, "thexi" MLCT state, which may be emissive and has a square planar-like geometry, labeled SP*.[26] Radiative relaxation is vertical in a Franck−Condon sense and the product must maintain the same nuclear coordinates and hence geometry of the "thexi" state. In other words, *radiative decay does not yield the ground state but rather a thermodynamically unstable isomer that will subsequently distort to yield the true ground state*. This final photodriven isomerization process has not been observed, although it is a necessary and novel feature of copper diimine excited states. Nonradiative decay, on the other hand, can proceed directly to the T_d ground state from the SP* "thexi" state or it may follow the same pathway as radiative decay. It is not possible to quantify the discrete nonradiative rate constants for these different pathways from our measurements.

(24) The use of four discrete energy levels is a simplification, and in many cases a manifold of states are expected; see, for example, ref 26. Nevertheless, for the discussion at hand, this simplified model adequately describes the key points and the inclusion of multiple states for each level would not change the main conclusions.

(25) Damrauer, N. H.; Cerullo, G.; Yeh, A.; Boussie, T. R.; Shank, C. V.; McKusker, J. K. *Science* **1997**, *275*, 54.

(26) For $[Cu(\mathbf{1b})]^{2+*}$, temperature-dependent photophysical measurements have revealed that the "thexi" state is comprised of two MLCT states, separated in energy by ~ 1800 cm^{-1}, that behave as one state at room temperature: Kirchoff, J. R.; Gamache, R. E.; Blaskie, M. W.; Del Paggio, A. A.; Lengel, R. K.; McMillin, D. R. *Inorg. Chem.* **1983**, *22*, 2380.

The excited state lifetimes are controlled by nonradiative decay which is known to follow the energy gap law: nonradiative rate constants decrease exponentially with increasing magnitude of the energy separation between the ground and excited states.[27] Therefore, the key to achieving longer lived excited states is to increase the energy gap between the SP* state and the T_d and SP states in Figure 6. This can be achieved by minimizing the inner-sphere reorganization that accompanies the $T_d^* \rightarrow SP^*$ and the $SP \rightarrow T_d$ processes; i.e., minimize structural change before and after light emission. Therefore, a ground state Cu(I) coordination environment that is structurally similar to the emissive excited state, while maintaining a significant energy gap, is needed. The BHQ ligands accomplish exactly this requirement by providing considerable steric congestion in the vicinity of chelation, which stabilizes Cu(I), while also providing interligand π-stacking that distorts the ground-state geometry and favors photo-oxidation of the metal with little structural change. The small "Stokes-like" shift for $[Cu(\mathbf{5a-c})_2]^+$ is direct evidence of minimal inner-sphere reorganization.[28] Most luminescent $Cu(phen)_2^+$ complexes have a large, 800−1000 meV, difference between the absorption and emission maxima. In sharp contrast, the corresponding shifts for $[Cu(\mathbf{5a-c})_2]^+$ are only ∼200−300 meV. This relatively small Stokes-like shift coupled with the crystallographic data for $[Cu(\mathbf{5c})_2]^+$ support the model proposed and the observations reported by Karpishin.[4]

An additional benefit of π stacking and steric congestion is that it protects the copper center from coordinating solvents and counterions. Lewis basic molecules and ions are known to quench the excited states of copper diimine compounds, which is unwanted for many applications. McMillin has proposed an exciplex quenching model where the coordination number of copper in the excited state increases to five promoting rapid nonradiative decay.[29] The $[Cu(\mathbf{5a-b})_2]^{+}$* complexes are highly luminescent in coordinating solvents such as CH_3CN but, their lifetimes are decreased from what is observed in CH_2Cl_2 suggestive of inefficient exciplex quenching. Nevertheless, the excited states of $[Cu(\mathbf{5a-b})_2]^+$ could be utilized for applications in sensing or photocatalysis where diffusional quenching is required.

Conclusions

Two series of 3,3′-polymethylene bridged bipyridines have been synthesized involving naphtho[1,2-*b*] fusion to one or both of the pyridines. Despite considerable congestion in the coordinating pocket, these ligands complex readily with Cu(I). The BHQ complexes $[Cu(\mathbf{5a-c})_2]^+$ are particularly interesting in that both solution and solid-state analysis evidence considerable $\pi-\pi$ interaction between the BHQ rings of opposing ligands. This same series of complexes evidences strong MLCT absorption and room-temperature luminescence in CH_2Cl_2 solution. The tetramethylene-bridged BHQ complex $[Cu(\mathbf{5c})_2]^+$ shows the longest excited-state lifetime yet observed for a Cu(I) complex (5.3 μs). Thus highly congested or crowded ligands such as bi-BHQ may form well organized Cu(I) complexes which accommodate highly distorted coordinative bonds but profit from stabilization associated with π-stacking interactions.

Acknowledgment. R.P.T. thanks the Robert A. Welch Foundation and the National Science Foundation (CHE-9714998) and D.V.S. and G.J.M. acknowledge the donors of the Petroleum Research Fund, administered by the ACS, for financial support of this work. E.C.R. thanks the NIGMS of the NIH for a National Research Service award (GM 17191-03). We also thank Professor Deborah Roberts for assistance with the electrospray mass spectra, Dr. James Korp for assistance with the X-ray determinations, and Professor Raymond Ziessel for stimulating discussion.

Supporting Information Available: X-ray crystallographic files in CIF format for $[Cu(\mathbf{4})_2](ClO_4)$ and in PDF format for $[Cu(\mathbf{5c})_2](ClO_4)$. The material is available free of charge via the Internet at http://pubs.acs.org.

IC010297H

(27) (a) Freed, K. F.; Jortner, J. *J. Chem. Phys.* **1970**, *52*, 6272. (b) Kober, E. M.; Caspar, J. V.; Lumpkin, R. S.; Meyer, T. J. *J. Phys. Chem.* **1983**, *87*, 952.

(28) The Stokes shift for these complexes would be the energetic separation between the singlet-to-triplet absorption and the emission. Since this absorption band has not been identified, we use the term "Stokes-like" shift and emphasize that this is a crude approach useful for comparative purposes.

(29) (a) McMillin, D. R.; Kirchoff, J. R.; Goodwin, K. V. *Coord. Chem. Rev.* **1985**, *64*, 83. (b) Palmer, C. E. A.; McMillin, D. R.; Kirmaier, C.; Holten, D. *Inorg. Chem.* **1987**, *26*, 3167. (c) Stacy, E. M.; McMillin, D. R. *Inorg. Chem.* **1990**, *29*, 393.